Grüneisen Gamma of Some Cubic Crystals from Third-Order Elastic Constants Data

by **R. Ramji Rao**[1]) and **M. Peter**

Institute of Physics of Condensed Matter, University of Geneva, Geneva, Switzerland

(30. VIII. 74)

Abstract. A simple procedure is described to calculate the generalized Grüneisen parameters for longwave acoustic modes in cubic crystals from third-order elastic constants data. This procedure is used to calculate the limits $\bar{\gamma}_L$ and $\bar{\gamma}_H$ of the Grüneisen gamma of sixteen cubic crystals for which the measured third-order elastic constants are available. The agreement between the calculated limits and the experimental values from thermal expansion data is, in general, good. It is found that the alkali halides NaCl and NaF confirm Barron's predictions and the unusual behaviour of KCl and LiF is discussed within the framework of negative mode gammas. In the alkaline-earth fluorides CaF_2 and BaF_2 the elastic $\bar{\gamma}_H$ is found to be smaller than the thermal $\bar{\gamma}_H$ indicating a large contribution to $\bar{\gamma}_H$ from optical modes at high temperatures for these fluorides. In silver, gold and aluminium, farther neighbour interactions appear to be predominant. In indium antimonide, the calculated $\bar{\gamma}_L$ is negative which is, perhaps, suggestive of the experimental fact of the existence of a negative thermal expansion region at low temperatures for this insulator.

1. Introduction

Thermal expansion is a direct consequence of the anharmonicity of the lattice and is calculated from the anharmonic terms in the power series expansion of the crystal potential energy. In cubic crystals, a measure of this anharmonicity is the Grüneisen gamma defined by

$$\bar{\gamma}(T) = \frac{\beta V}{\chi C_v} = \frac{\sum_i \gamma_i C_{vi}}{\sum_i C_{vi}} \tag{1.1}$$

where β is the volume coefficient of expansion, V the molar volume, χ the isothermal compressibility and C_v is the specific heat at constant volume. The Grüneisen gamma is also sometimes designated as an effective Grüneisen function or as a thermodynamic parameter. The right-hand term of equation (1.1) gives the microscopic significance of $\bar{\gamma}(T)$ in the quasi-harmonic approximation. γ_i is the microscopic mode gamma or the generalized Grüneisen parameter (GP) associated with the ith normal mode frequency

---

[1]) On leave from the Department of Physics, Indian Institute of Technology, Madras-600036, India.

ω_i of the lattice and is defined by the equation

$$\gamma_i = -\frac{d \ln \omega_i}{d \ln V} \qquad (1.2)$$

The microscopic γ_i, in the quasi-harmonic approximation, is independent of temperature. The Grüneisen gamma is a weighted average of the individual γ_i's, the weighting factors being the C_{vi}, the constant-volume specific heat contribution of the ith normal frequency ω_i of the lattice. The Grüneisen gamma is temperature dependent through the temperature variation of the weighting factors, the C_{vi} being a measure of the degree of excitation of the mode. It follows that γ should remain constant after all the modes are completely excited and this is the high temperature limit $\bar{\gamma}_H$. At very low temperatures the thermal expansion coefficient of any crystal is mainly determined by the elastic modes of the lattice and their dependence on the strains of the lattice. For isotropic and cubic materials it is enough to consider the dependence of the frequency on the volume strain. For elastic waves in isotropic or cubic materials, γ_i would depend on the polarization and direction of propagation of the wave. At very low temperatures, the number of normal modes excited in the jth acoustic branch is proportional to $v_j^{-3}(\theta, \phi)$, v_j being the wave velocity. So the Grüneisen gamma, at very low temperatures (T^3 region), is again a constant designated as $\bar{\gamma}_L$ and is given by

$$\gamma_L = \frac{\sum\limits_{i=1}^{3} \int \gamma_i(\theta, \phi)\, V_i^{-3}(\theta, \phi)\, d\Omega}{\sum\limits_{i=1}^{3} V_i^{-3}(\theta, \phi)\, d\Omega} \qquad (1.3)$$

where Ω is the solid angle. The low temperature limit $\bar{\gamma}_L$ can be calculated from the individual GPs (γ_i's) of the elastic modes. In this paper, a simple method is presented to calculate the individual mode gammas γ_i for the elastic waves propagating in cubic crystals from a knowledge of the third-order elastic (TOE) constants of the crystal and hence the low and high temperature limits are evaluated. This has been done for sixteen crystals for which experimental TOE constants are available.

2. Method of Evaluating the GPs for Elastic Modes

The equation for elastic wave propagation in a homogeneously deformed crystal is given by Thurston and Brugger [1] as

$$\rho_0 w^2 u_i = \sum_{j,\, kl} A^S_{ij,\, kl} N_k N_l u_j \qquad (2.1)$$

Here ρ_0 is the density of the crystal in the undeformed state and w is the natural wave velocity in a direction having direction cosines N_k in the undeformed state and is given by $2L_0/t$ where L_0 is the zero-pressure length of the soundpath and 't' is the round-trip sound travel time. u_j are the components of displacement from the strained state. To the first order in strain, $A^S_{ij,\, kl}$ is given by

$$A^S_{ij,\, kl} = C^S_{ik,\, jl} + \sum_{mn} (C_{ik,\, jl,\, mn} + C_{kl,\, mn} \delta_{ij} + C_{ik,\, nl} \delta_{mj} + C_{nk,\, jl} \delta_{mi})\, \epsilon_{mn} \qquad (2.2)$$

The $C^S_{ik,jl}$ are the adiabatic second-order elastic (SOE) constants in the undeformed state and $C_{ik,jl,mn}$ are the third-order elastic (TOE) moduli in Brugger's notation determined by measuring the changes in wave velocity under isothermal strain. ϵ_{mn} are the deformation parameters. It may be mentioned that the initial strain is obtained by isothermal deformation. So the coefficients of ϵ_{mn} are isothermal coefficients. A cubic crystal subjected to a hydrostatic pressure, P, will experience a uniform volume strain ϵ (negative) and we have for ϵ_{mn} in equation (2.2)

$$\epsilon_{xx} = \epsilon_{yy} = \epsilon_{zz} = \left(-\frac{\epsilon}{3}\right); \quad \epsilon_{ij} = 0 \quad \text{when } i \neq j \tag{2.3}$$

The values of $\rho_0 w^2(\epsilon)$ can be found as the eigenvalues of equations (2.1). We need to know $w^2(0)$ and $dw^2/d\epsilon$. Hence we diagonalize the matrix

$$\mathbf{C} = [C_{ij}] \quad \text{where } C_{ij} = \sum_{kl} C^S_{ij,kl} N_k N_l \tag{2.4}$$

by means of Jacobi's method to get the matrix $\mathbf{A}$ and the corresponding transforming matrix $\mathbf{u}$:

$$\mathbf{A} = \tilde{\mathbf{U}} \times \mathbf{C} \times \mathbf{U} \quad \text{with } A_{ii} = (i); \quad (i = 1, 2, 3) \tag{2.5}$$

Next we transform the matrix

$$\mathbf{D} = [D_{ij}];$$
$$D_{ij} = -\tfrac{1}{3} \sum_{kl,n} N_k N_i (C_{ij,kl,nn} + C_{kl,nn}\delta_{ij} + C_{ik,nl}\delta_{nj} + C_{nk,jl}\delta_{ni}) \tag{2.6}$$

to get

$$\left.\begin{aligned} \mathbf{B} &= \tilde{\mathbf{U}} \times \mathbf{D} \times \mathbf{U} \\ \text{with} \quad & \\ B_{ii} &= Y(i) \end{aligned}\right\} \tag{2.7}$$

Here

$$N_x = \sin\theta \cos\phi$$
$$N_y = \sin\theta \sin\phi$$
$$N_z = \cos\phi \tag{2.8}$$

θ is the polar angle which the wave-vector makes with the Z-axis and ϕ is the azimuthal angle which the projection of the wave-vector in the basal plane makes with the X-axis. Then we have

$$Y(i) = \frac{\partial}{\partial\epsilon} X_i \tag{2.9}$$

and

$$\gamma_i \frac{-Y(i)}{2X_i} \quad (i = 1, 2, 3) \tag{2.10}$$

Knowing the individual γ_i's, $\bar{\gamma}_L$ is evaluated from the formula

$$\bar{\gamma}_L = \frac{\sum_{i=1}^{3} \int \gamma_i X_i^{-3/2} \, d\Omega}{\sum_{i=1}^{3} \int X_i^{-3/2} \, d\Omega} \tag{2.11}$$

A rigorous calculation of $\bar{\gamma}_H$ is possible only when all the γ_i's are known. In the present method we have only the γ_i's of the low frequency non-dispersive modes and not the high-frequency γ_i's. However, one can estimate an approximate $\bar{\gamma}_H$ as, in the Debye approximation, the high temperature limit is the mean value of the γ_i's over the elastic waves propagating in all directions. The approximate $\bar{\gamma}_H$ is also calculated for all the sixteen crystals in this way. The $\bar{\gamma}_L$ and $\bar{\gamma}_H$ values for the various crystals are evaluated numerically using HP 9830A calculator. The program sampled 478 points, over the irreducible spherical triangle, of the wave-directions.

3. Input Data and Results

For the calculation of the microscopic gammas we need, as mentioned above, the experimental SOE and TOE constants of the cubic crystals and these are given in Tables I and II. The values of the SOE and TOE constants of all the crystals with the exception of germanium are those at room temperature and the values for germanium are at 77°K. The TOE constants of copper at 4.2°K measured by Salama and Alers [2] are not used in the present calculations as the authors themselves mention in their paper that the TOE constants C_{111} and C_{123} need adjustment to get the appropriate value of $\bar{\gamma}_L$. $d(C_{11} - C_{12})/dP$ and dC_{44}/dP are not accurately determined by their low temperature measurements of the TOE constants. The limits of gamma for GaAs have been evaluated using the TOE constants data of both Drabble and Brammer [8a] and of McSkimmin and Andreatch [8b]. The values of $\bar{\gamma}_L$ and $\bar{\gamma}_H$ for the sixteen crystals

Table I
SOE constants in 10^{11} dynes/cm²

S. No.	Crystal	C_{11}	C_{12}	C_{44}	Authors and reference
1	Copper	16.61	11.99	7.56	Hiki and Granato [3]
2	Silver	12.22	9.07	4.54	Hiki and Granato [3]
3	Gold	19.29	16.38	4.15	Hiki and Granato [3]
4	Aluminium	10.675	6.041	2.834	Thomas Jr. [4]
5	Nickel	25.03	15.11	12.24	Sarma and Reddy [5]
6	Germanium	13.112	4.923	6.817	McSkimmin and Andreatch [6]
7	Silicon	16.577	6.392	7.962	McSkimmin and Andreatch [7]
8	GaAs	i) 11.904	i) 5.384	i) 5.952	i) Drabble and Brammer [8a]
		ii) 11.877	ii) 5.372	ii) 5.944	ii) McSkimmin and Andreatch [8b]
9	InSb	6.700	3.649	3.019	Drabble and Brammer [9]
10	NaCl	4.942	1.269	1.281	Drabble and Strathen [10]
11	KCl	4.090	0.704	0.627	Drabble and Strathen [10]
12	LiF	11.397	4.767	6.364	Drabble and Strathen [10]
13	NaF	9.68	2.42	2.80	Bensch [11]
14	CaF$_2$	16.42	4.398	3.370	Wong and Schuele [12]
15	BaF$_2$	8.948	3.854	2.495	Gerlich [13]
16	RbMnF$_3$	11.740	4.214	3.193	Melcher and Bolef [14]

Table II

TOE constants in 10^{11} dynes/cm^2

S. No.	Crystal	C_{111}	C_{112}	C_{123}	C_{144}	C_{166}	Authors and reference
1	Copper	−127.1	−81.4	−5.0	−0.3	−78.0	Hiki and Granato [3]
2	Silver	−84.3	−52.9	+18.9	+5.6	−63.7	Hiki and Granato [3]
3	Gold	−172.9	−92.2	−23.3	−1.3	−64.8	Hiki and Granato [3]
4	Aluminium	−107.6	−31.5	+3.6	−2.3	−34.0	Thomas Jr. [4]
5	Nickel	−210.4	−134.5	+5.9	−18.0	−75.7	Sarma and Reddy [5]
6	Germanium	−76.0	−41.0	−7.0	0.0	−31.0	Drabble and Fendley [15]
7	Silicon	−82.5	−45.1	−6.4	+1.2	−31.0	McSkimmin and Andreatch [16]
8	GaAs	i) −67.5	i) −40.2	i) −0.4	i) −7.0	i) −32.0	i) Drabble and Brammer [8a]
		ii) −62.2	ii) −38.7	ii) −5.7	ii) +0.2	ii) −26.9	ii) McSkimmin and Andreatch [8b]
9	InSb	−31.4	−21.0	−4.8	+0.9	−11.8	Drabble and Brammer [9]
10	NaCl	−84.3	−5.0	+4.6	+2.9	−6.0	Drabble and Strathen [10]
11	KCl	−72.6	−2.4	+1.1	+2.3	−2.6	Drabble and Strathen [10]
12	LiF	−142.3	−26.4	+15.6	+8.5	−27.3	Drabble and Strathen [10]
13	NaF	−148.0	−27.0	+28.0	+4.6	−11.4	Bensch [11]
14	CaF$_2$	−124.6	−40.0	−25.4	−12.4	−21.4	Alterovitz and Gerlich [17]
15	BaF$_2$	−58.4	−29.9	−20.6	−12.1	−8.89	Gerlich [13]
16	RbMnF$_3$	−184.0	−24.0	+4.0	−6.0	−18.0	Naimon and Granato [18]

Table III
Calculated values of $\bar{\gamma}_H$ and $\bar{\gamma}_L$ and comparison with experimental values

S. No.	Crystal	Present calculations		$\bar{\gamma}_L^{expt}$ and reference	$\bar{\gamma}_H^{expt}$ and reference	Calculated value of others	
		$\bar{\gamma}_L$	$\bar{\gamma}_H$			$\bar{\gamma}_L^{others}$ and reference	$\bar{\gamma}_H^{others}$ and reference
1	Cu	1.765	2.032	1.72 ± 0.03 [19] 1.76 [20]	2.0 [19] 1.97 [22] 2.03 [25]	1.77 [21]	1.98 [21] 2.07 [23] 1.97 [25]
2	Ag	2.493	2.498	2.2 ± 0.1 [21] 2.63 ± 0.16 [24] at 20°K	2.4 [21] 2.48 [25] 2.46 [22]	2.22 [21]	2.4 [21] 2.55 [23] 2.40 [25]
3	Au	2.582	2.574	3.50 ± 0.22 [24] at 12°K	3.0 ± 0.06 [21] 2.90 [25] 3.09 [22]	2.92 [21] 2.20 ± 0.6 [23]	3.04 [21] 3.02 [25] 2.65 [23]
4	Al	2.265	2.216	2.65 ± 0.15 [21] 2.45 [4]	2.34 [21] 2.19 [4] 2.18 [22]	2.62 [21] 2.33 [4]	2.58 [21] 2.27 [4]
5	Ni	1.410	1.613	—	2.0 [22] 1.88 ± 0.08 [22]	—	—
6	Ge	0.504	0.757	0.45 at 8°K [27] 0.655 ± 0.01 [28] 0.50 [30]	0.625 at 130°K [27] ~0.72 [21] 0.80 [22] ~0.75 [30] 0.72 [32]	0.49 [26] 0.48 [21] ~0.52 [29]	0.71 [21] 0.76 [31] ~0.75 [29] 0.76 [28]
7	Si	0.250	0.489	0.25 [30] 0.38 at 12°K [27] 0.437 ± 0.01 [28]	0.446 at 280°K [27] 0.44 [21] 0.57 [22] 0.43 [30] 0.48 [32]	0.25 [21] 0.251 [29] 0.24 ± 0.02 [36] 0.21 [36]	0.54 [21] 0.50 [29] 0.45 [28]
8	GaAs	i) 0.735 using Drabble and Brammer values ii) 0.369 using McSkimmin and Andreatch values	0.994 0.654	0.583 (± 0.01) [28]	0.75 [32]	—	1.0 [28]

Table III (*continued*)

S. No.	Crystal	Present calculations		$\bar{\gamma}_L^{expt}$ and reference	$\bar{\gamma}_H^{expt}$ and reference	Calculated value of others	
		$\bar{\gamma}_L$	$\bar{\gamma}_H$			$\bar{\gamma}_L^{others}$ and reference	$\bar{\gamma}_H^{others}$ and reference
9	InSb	−0.006	0.334	0.21 ± 0.01 [28] −0.022 at 14°K [33]	0.55 [32]	—	0.55 [28]
10	NaCl	1.168	1.463	0.93 ± 0.03 [21] 0.94 [34] 0.90 ± 0.03 [35] 0.94 [35] 1.04 [52]	1.55 [21, 34] 1.60 [25] 1.57 [35] 1.59 [37] 1.58 ± 0.01 [38] 1.06 [52]	1.22 [21] 1.23 [25] 1.25 [29] 1.09 [34] 1.05 [35] 0.95 ± 0.1 [39]	1.61 [21] 1.60 [25] 1.53 [29] 1.51 [34] 1.59 ± 0.01 [39]
11	KCl	0.437	1.255	0.32 ± 0.03 [21] 0.32 ± 0.02 [35] 0.34 [34] 0.324 [40] 0.35 [52]	1.47 [21] 1.45 [35] 1.50 [34] 1.44 [40] 1.48 [25] 1.46 [37] 1.45 ± 0.01 [38]	0.525 [25] 0.43 [21] 0.531 [29] 0.31 [34] 0.34 ± 0.03 [39] 0.33 [52]	1.37 [25] 1.25 [21] 1.28 [29] 1.06 [34] 1.44 ± 0.01 [39]
12	LiF	1.403	1.243	1.7 [52] 1.70 ± 0.05 [35] 1.60 at 60°K [37]	1.58 [35] 1.59 [37] 1.63 [41]	1.85 [35] 1.92 [29] 1.65 [52]	1.66 [35, 29, 42] 1.72 [41]
13	NaF	1.228	1.540	0.92 [52]	—	1.13 [29] 0.99 [52] 1.02 [52]	1.44 [29] 1.39 [42] 1.55 [11] 1.21 [45]
14	CaF$_2$	0.933	1.128	1.2 ± 0.2 [43] ($T < 10°K$) 0.8 ± 0.5 [44]	1.90 at 280°K [43] 1.88 at 270°K [44]	1.08 [45] 0.84 [46] 3.06 [47]	
15	BaF$_2$	0.346	0.739	0.2 ± 0.4 [44]	1.57 at 270°K [44]	0.38 ± 0.03 [13] 0.26 [45] −0.03 [46]	0.77 ± 0.05 [13] 0.70 [45]
16	RbMnF$_3$	1.713	1.874	—	—	—	—

Table IV

$(\bar{\gamma}_H - \bar{\gamma}_L)$ for the sixteen crystals

S. No.	Crystal	$(\bar{\gamma}_H - \bar{\gamma}_L)$ (calculated)
1	Cu	0.267
2	Ag	0.005
3	Au	−0.008
4	Al	−0.049
5	Ni	0.203
6	$RbMnF_3$	0.161
7	Ge	0.253
8	Si	0.239
9	GaAs	i) 0.259
		ii) 0.285
10	InSb	0.340
11	NaCl	0.295
12	KCl	0.818
13	LiF	−0.160
14	NaF	0.312
15	CaF_2	0.195
16	BaF_2	0.393

calculated by using the procedure outlined in Section 2 are given in Table III and compared with the available experimental measurements as well as with the calculations of others, if any. Table IV shows the differences between the calculated $\bar{\gamma}_H$ and $\bar{\gamma}_L$ values.

4. Discussion

Considering the noble metals copper, silver and gold, the agreement between the present calculated values and the experimental thermal values is good for copper and silver. In the case of gold the $\bar{\gamma}_L$ experimental value is the one at 12°K and possibly below 12°K this value may further decrease. Barron [48] predicts for a fcc lattice a value of 0.3 for the difference between the high and low temperature limits of gamma for nearest-neighbour central interactions and a decrease of this value when farther neighbours also interact. Following this, one finds from our calculations that a nearest-neighbour central-force model holds good for copper while this is not true for silver and gold. The recent lattice dynamical studies of gold by Lynn et al. [49] lend support to this fact. Aluminium also falls into the category of gold in having farthest neighbour interactions and the agreement between calculation and measurement of the limits of gamma is excellent. We do not find the low temperature thermal expansion measurements for the magnetic materials nickel and $RbMnF_3$. For nickel, the calculated $\bar{\gamma}_H$ value differs from the value given by Gschneidner [22] by 15%.

In germanium and silicon our calculated values of $\bar{\gamma}_L$ and $\bar{\gamma}_H$ are in fair agreement with the values of McCammon and White [30] while the $\bar{\gamma}_L$ values reported by Sparks and Swenson [28] are consistently larger. This has been pointed out by Beattie and Shirber [36] also whose calculated $\bar{\gamma}_L$ value for silicon (0.24 ± 0.02) agrees with our value of 0.25. In GaAs, we calculated the limits of the Grüneisen gamma using the measured TOE constants of i) Drabble and Brammer [8a] and ii) McSkimmin and Andreatch [8b]. Our calculated value with either of these set of TOE constants for GaAs does not agree with the measured value of Sparks and Swenson [28] and agrees

with the value of Novikova [32] to within 15%. In indium antimonide, the calculated $\bar{\gamma}_L$ value shows a negative trend when $\bar{\gamma}_L$ is considered to the third decimal. It is an established experimental fact that at low temperatures (T^3 region) these semiconducting materials germanium, silicon, gallium-arsenide and indium antimonide have a range of negative values of gamma ($\bar{\gamma}$) which coincides with the region of negative expansion coefficient. With a further decrease of the temperature these low $\bar{\gamma}$ values tend to be positive and ultimately the $\bar{\gamma}_L$ values become positive only. The negative sign of the calculated $\bar{\gamma}_L$ value for InSb is, perhaps, indicative of the fact that there is a low temperature region in which the thermal expansion becomes negative for this semiconducting material. Also it appears that in these diamond structure semiconducting materials, which have a strong covalent bonding, nearest-neighbour central interactions play a predominant role.

Among the alkali halides, we may put NaCl and NaF in one group and KCl and LiF in the second group in discussing their thermal behaviour. NaCl and NaF are the normal alkali halides in the sense that the Grüneisen gamma decreases gradually with decreasing temperature and the difference between the high and low temperature limits is not abnormal. When a low γ_i is associated with a low stiffness mode, it would be weighted very heavily according to the equation $\bar{\gamma} = \sum C_i \gamma_i / \sum C_i$ at low temperatures but not at high temperatures. And the $\bar{\gamma}$ would then be expected to fall at low temperatures. This is precisely the situation for NaCl and NaF which have low γ_i's (some of them are negative with small magnitudes) associated with low stiffness modes. As a matter of fact, these two materials obey Barron's predictions and fit into the scheme of a nearest-neighbour central-force model. Our calculated value of $\bar{\gamma}_L$ for NaF is larger than the recently measured thermal value of White and Collins [52]. For NaF there is no experimental data on $\bar{\gamma}_H$. However, our calculated values are in line with the calculated values of Brugger and Fritz [29] and of Bensch [42]. In NaCl, our values are as much in good agreement with the experimental values as those calculated by others (see Table III). In KCl the agreement between calculation and measurement is within 25%. More than this, we find that the difference between $\bar{\gamma}_H$ and $\bar{\gamma}_L$ for KCl is quite large. This situation in KCl is similar to that in RbI [50]. The values of γ_i for the acoustic modes in the non-dispersive region obtained from the experimental TOE constants in general vary with the type of normal mode vibration and this variation with mode type is particularly wide in KCl. In this alkali halide, over most of the θ, ϕ range a very low value of γ_i is associated with the lowest velocity mode which is determined principally by the elastic stiffness constant C_{44} and (C_{44} is small for KCl). Indeed, in KCl the lowest velocity mode has a negative γ_i (with large magnitude) in certain directions. Because the low velocity modes are heavily weighted at low temperatures, we find for KCl that the averaged Grüneisen constants calculated from the elastic data have the relation $\gamma_L \ll \gamma_H$. A word about these negative mode Grüneisen parameters for some of the TA modes of KCl and NaCl; a negative γ_{TA} indicates a decrease in the stiffness of the lattice under compression predicting a first-order transition [51]. It is well known that NaCl-type crystals undergo a pressure – induced phase – transition to the CsCl structure and this fact is not obscured by our present calculations. In LiF we find $\bar{\gamma}_L$ calculated is slightly greater than $\bar{\gamma}_H$ calculated and both our $\bar{\gamma}_L$ and $\bar{\gamma}_H$ values are off from the measured values by 15% and 20% respectively. The shear constant C_{44} has a large value for LiF and the lowest γ_i is associated with this high stiffness mode and is not heavily weighted at low temperatures. So we might expect the gamma to rise at low temperatures which is reflected in the computed results for LiF where $\bar{\gamma}_L$ is greater than $\bar{\gamma}_H$ although by a small amount.

In the alakaline-earth fluorides CaF_2 and BaF_2, the calculated $\bar{\gamma}_L$ values are in good agreement with the measured $\bar{\gamma}_L$ values if one takes into account the errors involved in these low temperature measurements. The elastic $\bar{\gamma}_H$ values for these two
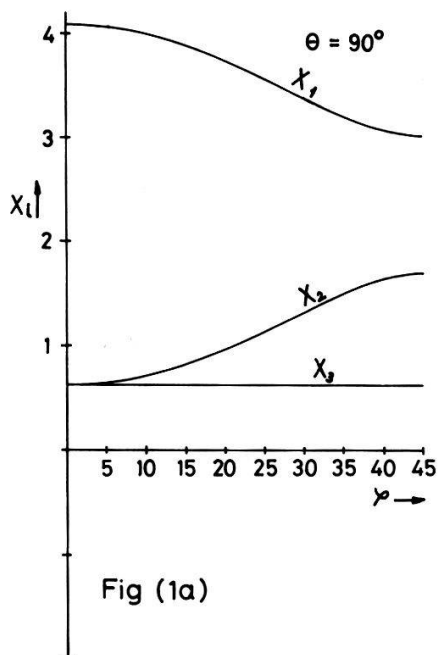

Figure 1a
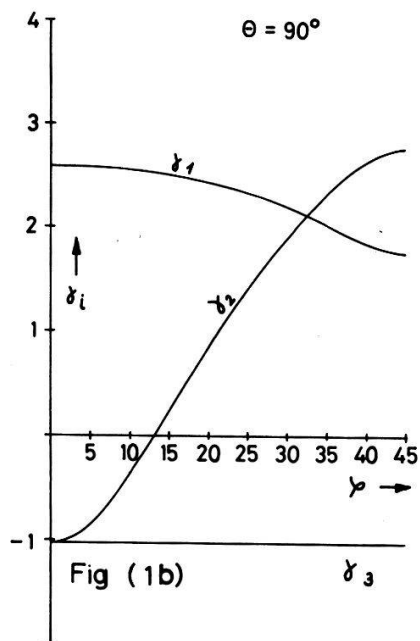Plot of $\chi_i = \rho_0 v_i^2$ versus ϕ for KCl for $\theta = 90°$. Here X_3 is the low shear-mode velocity.

Figure 1b
Plot of γ_i versus ϕ for KCl for $\theta = 90°$. Here γ_3 is associated with X_3.

fluorides are considerably different from the measured $\bar{\gamma}_H$ values. Our calculated values, however, agree reasonably with the calculated values of Gerlich [13] (BaF_2) and those of Srinivasan [46] and of Wong and Schuele [45] (CaF_2). In both CaF_2 and BaF_2 the disagreement for $\bar{\gamma}_H$ is much larger than for $\bar{\gamma}_L$, the elastic $\bar{\gamma}_H$ being lower than than the thermal value. We may conclude that at high temperatures, in both CaF_2 and BaF_2, the contributions of the optical modes to the γ_i's become significant. Finally, as

an example, the graphs of $(X_i - \phi)$ and $(\gamma_i - \phi)$ are given in Figures 1a and 1b for $\theta = 90°$ in KCl to show the negative values of γ_i associated with the low-velocity transverse acoustic modes.

REFERENCES

[1] R. N. Thurston and K. Brugger, Phys. Rev. 133, 1604 (1964).
[2] K. Salama and G. A. Alers, Phys. Rev. 161, 673 (1967).
[3] Y. Hiki and A. V. Granato, Phys. Rev. 144, 411 (1966).
[4] J. F. Thomas, Jr., Phys. Rev. 175, 955 (1968).
[5] V. P. N. Sarma and P. J. Reddy, Phil. Mag. 27, 769 (1973).
[6] H. J. McSkimmin and P. Andreatch, Jr., J. Appl. Phys. 34, 651 (1963).
[7] H. J. McSkimmin and P. Andreatch, Jr., J. Appl. Phys. 35, 2161 (1964).
[8] a) J. R. Drabble and A. J. Brammer, Solid State Comms 4, 467 (1966); b) H. J. McSkimmin and P. Andreatch, Jr., J. Appl. Phys. 38, 2610 (1967).
[9] J. R. Drabble and A. J. Brammer, Proc. Phys. Soc. 91, 959 (1967).
[10] J. R. Drabble and R. E. B. Strathen, Proc. Phys. Soc. 92, 1090 (1967).
[11] W. A. Bensch, Phys. Rev. B 6, 1504 (1972).
[12] C. Wong and D. E. Schuele, J. Phys. Chem. Solids 28, 1225 (1967).
[13] D. Gerlich, Phys. Rev. 168, 947 (1968).
[14] R. L. Melcher and D. L. Bolef, Phys. Rev. 178, 864 (1969).
[15] J. R. Drabble and J. Fendley, J. Phys. Chem. Solids 28, 669 (1967).
[16] H. J. McSkimmin and P. Andreatch, Jr., J. Appl. Phys. 35, 3312 (1964).
[17] S. Alterovitz and D. Gerlich, Phys. Rev. 184, 999 (1969).
[18] E. R. Naimon and A. V. Granato, Phys. Rev. B 7, 2091 (1973).
[19] R. H. Carr, R. D. McCammon and G. K. White, Proc. Roy. Soc. (London) A 280, 72 (1964).
[20] R. H. Carr and C. A. Swenson, Cryogenics 4, 76 (1964).
[21] J. G. Collins, Phil. Mag. 8, 323 (1963).
[22] K. A. Gschneidner, Jr., Solid State Phys. 16, 414 (1964).
[23] Y. Hiki, J. F. Thomas, Jr. and A. V. Granato, Phys. Rev. 153, 764 (1967).
[24] D. B. Fraser and A. C. Hollis Hallett, Can. J. Phys. 43, 193 (1965).
[25] F. W. Sheard, Phil. Mag. 3, 1381 (1958).
[26] W. B. Daniels, Phys. Rev. Letters 8, 3 (1962).
[27] R. H. Carr, R. D. McCammon and G. K. White, Phil. Mag. 12, 157 (1965).
[28] P. W. Sparks and C. A. Swenson, Phys. Rev. 163, 779 (1967).
[29] K. Brugger and T. C. Fritz, Phys. Rev. 157, 524 (1967).
[30] R. D. McCammon and G. K. White, Phys. Rev. Letters 10, 234 (1963).
[31] G. K. White and S. B. Woods, Phys. Rev. 103, 569 (1956).
[32] S. I. Novikova, Soviet Physics-Solid State 7, 2170 (1966) (translation).
[33] D. F. Gibbons, Phys. Rev. 112, 136 (1958).
[34] D. E. Schuele and C. S. Smith, J. Phys. Chem. Solids 25, 801 (1964).
[35] G. K. White, Proc. Roy. Soc. Series A, 286, 204 (1965).
[36] A. G. Beattie and J. E. Shirber, Phys. Rev. B 1, 1548 (1970).
[37] B. Yates and C. H. Panter, Proc. Phys. Soc. 80, 373 (1962).
[38] P. P. M. Meincke and G. M. Graham, Can. J. Phys. 43, 1853 (1965).
[39] T. H. K. Barron, A. J. Leadbetter and J. A. Morrison, Proc. Roy. Soc. Series A, 279, 62 (1964).
[40] F. G. Awad and D. Gugan, Cryogenics 11, 414 (1971).
[41] R. Ruppin and R. W. Roberts, Phys. Rev. B 3, 1406 (1971).
[42] R. A. Miller and C. S. Smith, J. Phys. Chem. Solids 25, 1279 (1964).
[43] J. G. Collins and G. K. White, Prog. Low Temp. Phys. 4, 450 (1964).
[44] A. C. Bailey and B. Yates, Proc. Phys. Soc. 91, 390 (1967).
[45] C. Wong and D. E. Schuele, J. Phys. Chem. Solids 29, 1309 (1968).
[46] R. Srinivasan, J. Phys. C, Series 2, 1, 1138 (1968).
[47] S. Ganesan and R. Srinivasan, Can. J. Phys. 40, 91 (1962).
[48] T. H. K. Barron, Phil. Mag. 46, 720 (1955).
[49] J. W. Lynn, H. G. Smith and R. M. Nicklow, Phys. Rev. B 8, 3493 (1973).
[50] D. E. Schuele and C. S. Smith, J. Phys. Chem. Solids 25, 801 (1964).
[51] W. B. Daniels, in Lattice Dynamics, edited by R. F. Wallis (Pergamon Press, London 1965), p. 273.
[52] G. K. White and J. G. Collins, Proc. Roy. Soc. Series A, 333, 237 (1973).